

一九四八年五月九日日食與武昌 上空 F-2 層所受之影響

桂質廷 梁百先 莫紀華 周煒*

(武漢大學游離層實驗室)

這次日食的中心帶經過粵、贛、浙、蘇諸省入黃海。武昌雖不在環食帶上，在上空四百公里却有 $D = 0.833$ 的食分；食始在中原時間 0825，食甚在 0941，食終在 1105。

為研究日食對於游離層可能發生的影響，曾在九日上午 0700—1200，每 5 分鐘一次，觀測 F-2 層正常波的臨界頻率及視高度。靠近每點鐘時，則 E 與 F-1 層的頻率及視高度一併觀察；因此在食甚後 19 分鐘內缺少 F-2 層的重要資料。但是對於 E, F-1 兩層在日食時的變化獲得結果。為要與正常狀態相比較，在日食前後各 6 天同時間內每 15 分鐘觀測一次。但本文所取的平均值只限於 5 月 5 日及 14 日，其他 10 天地磁及游離層都表現不穩定情況。

本文主要結果可分以下部分：(1) 測定 F-2 層游子復合係數 $\alpha = 4 \times 10^{-10}$ 電子游子對/立方厘米秒；(2) 在日食時 F-2 層降低，其厚度減少；(3) 不規則 E 層非日光所產生；(4) 各游離層游子密度在日食時降低的估計。

略述方法如后：

I. 由日食時所得 $f_0 F_2 - t$ (臨界頻率——時間) 曲線與正常曲線相比，解

$$\frac{dN}{dt} = q_0 \cos \psi - \alpha N^2 \quad (1)$$

$$\left(\frac{dN}{dt} \right)_e = r q_0 \cos \psi - \alpha N_e^2 \quad (2)$$

式內 N, N_e 指在 t 時在平常及日食時之游子密度， ψ 為當時太陽的天頂角，

* 現在中國科學院地球物理研究所。

q_o 為太陽紫外線在 $F-2$ 層的游子密度產生率， r 為太陽未被遮的視平面與全視平面的百分比。所得的結果如下：

$$\alpha = (4.05 \pm .66) \times 10^{-10} \text{ 立方厘米/電子每秒}$$

$$q_o = (1.97 \pm .24) \times 10^3 \text{ 電子—游子對/立方厘米每秒}$$

然後解 (2) 為

$$N_2 = \frac{N_1 + q_o \frac{r_1 \cos \psi_1 + r_2 \cos \psi_2}{2} \Delta t}{1 + N_1 \alpha \Delta t} \quad (3)$$

取 $\alpha = 4 \times 10^{-10}$, $q_o = 2000$, 在初食時 (0826 中原時間) 觀測所得的游子密度 N_1 用公式 (3) 求 Δt 秒後的 N_2 ; 依次求平常與日食時不同時間的 N_1 及 N_2 得兩條理論曲線，其結果與觀測值頗相近似。在 1009 頻率陡增大概與東京天文台觀測的 0958 及 1017 的日冕噴射有關。

II. 取 $0.834 f_o F_2$ 的視高度與真高 (最大游子密度的高度)，再由觀測記錄推算 $F-2$ 層的最低視高度，二者之差應為 $F-2$ 層厚度之半。計算與圖解都證明在日食時層厚度減少，在日甚整個下降，以後又上升，大概是當日食時空氣溫度降低所致。

III. 在食始後 12 分起至食終後 38 分止，不斷有不規則 E 層存在，其最大頻率高至 12 百萬週波/秒，顯然不受日食時日光變化影響，故 E_s 層並非由日光直接產生。

IV. 此次日食武昌上空各游離層游子密度的降低率為 $F-2$ 層——31%
 $F-1$ 層——70%， E 層——60%。

THE F-2 REGION OF THE IONOSPHERE AT WUCHANG DURING THE SOLAR ECLIPSE OF MAY 9, 1948

By C. T. KWEI, P. H. LIANG, J. H. MOH, and W. CHOW*

Ionosphere Laboratory, Wuhan University, Wuchang

(Received July 30, 1951)

ABSTRACT

From data obtained during the eclipse and on control days, the effective coefficient of recombination for F-2 layer is found to be 4×10^{-10} cm³/electron per sec. The magnitude of α is apparently a function of the height of the layer which becomes lower with increasing latitude. Solar eruptions may be associated with two of the discontinuities of the eclipse curve. The thickness of the F-2 layer became compressed and dropped as a whole during the eclipse, possibly due to air movement caused by lowering of temperature. The sporadic E layer was not influenced by the change of solar radiation, and must be due to other causes.

Soon after the partial solar eclipse occurred over the Wuchang skies on May 9, 1948, one of us¹ made a preliminary report which was presented to the Assembly of the International Scientific Radio Union. In the present article, we wish to present a more detailed account and analysis of data obtained on that occasion.

As previously reported, the annular eclipse occurred over the south-eastern part of China, directly passing over portions of the provinces of Kwangtung, Kiangsi, Chekiang and Kiangsu. Here at Wuchang the eclipse would be 90.6%. At 400 km above ground level, the solar diameter obscured was 0.833 (solar diameter equal to unity). The eclipse began at 0825, reached its maximum at 0941 and ended at 1105 120° EMT. Because our equipment (DTM CIW Model 3) was manually operated and a full run to cover all layers would take 10 minutes or more, we limited our observations to the critical frequencies and virtual heights of the F-2 layer only, except when near the hour we took data for the complete run. This was unfortunate as it left a gap of 19 minutes shortly after the eclipse maximum unexplored. On the other hand we were enabled to study the effects of eclipse on the E and F-1 layers.

*Now at the Institute of Geophysics and Meteorology, Academia Sinica.

1. P. H. Liang, *URSI* 7 (1949), 247.

In order to obtain control data for comparison, observations were made from 0700 to 1200, 120° EMT, six days before and six days after May 9, that is from May 3 to May 15 inclusive. However, of these twelve days, only three were "international quiet days" magnetically, namely, May 4, 5, and 14 with international character figures 0.8, 0.4 and 0.5 respectively. As May 4 was rather disturbed with strong sporadic E blanketing up to 19.5 Mc from 0900 to 0930, we have only used the data for May 5 and 14 for comparison.

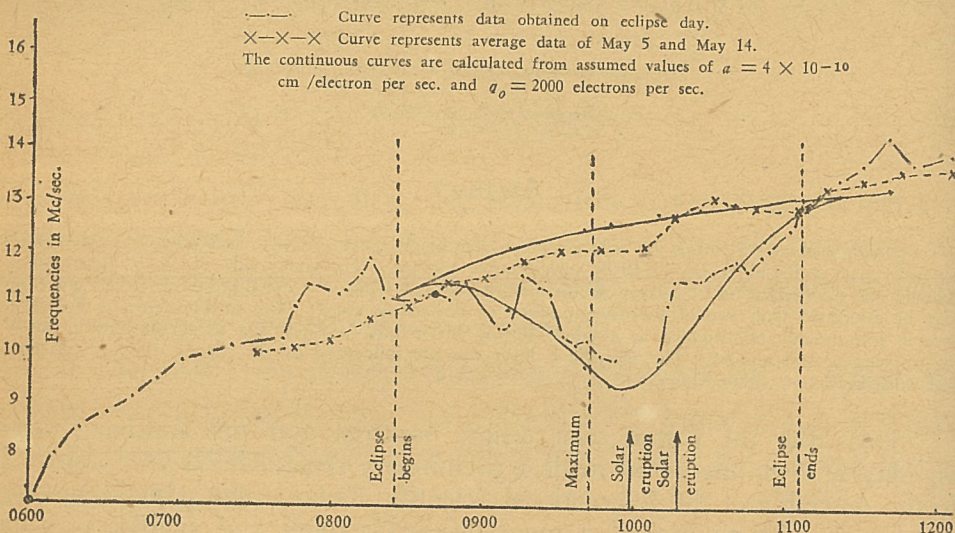


Fig. 1. Showing a distinct drop of F_2 critical frequencies during the solar eclipse at Wuchang, China, on May 9, 1948.

EFFECTIVE COEFFICIENT OF RECOMBINATION FOR F_2 LAYER FROM ECLIPSE DATA

The frequency *vs* time relationships are shown by curves in Fig. 1. The crosses are averaged data for May 5 and 14, and the dot and dash curve represents actual observations on the day of eclipse, and the continuous curves are calculated from theory showing the relationships with and without the eclipse effect by assuming the effective coefficient of recombination $\alpha = 4 \times 10^{-10}$ cm³/electron per sec, and the rate of production of ion when zenith angle is zero $q_0 = 2000$ ion-electron pairs/c.c. per sec.

It is seen that there is a definite drop in $f_0 F_2$ critical frequencies during the eclipse. On account of the unfortunate gap, we cannot accurately locate the time of the maximum drop, but it occurs somewhere between 9 and 28 minutes after the eclipse maximum (our theoretical curve locates it at about 13 minutes after the eclipse maximum). There is also a general trend of fall after the eclipse sets in and of recovery beyond the maximum drop. The recovery is complete within fifteen minutes after the eclipse ends. We are

therefore tempted to assume that solar photons and not corpuscles with slower velocities are largely responsible for the observed eclipse effects.

In arriving at our theoretical curves, we have adopted Hulbert's² simple treatment of the solar eclipse effect on the E layer. From the well known relationship

$$\frac{dN}{dt} = q - \alpha N^2 \quad (1)$$

Hulbert assumed that

$$q = q_0 \cos\psi \quad (2)$$

where q_0 has already been defined and ψ denotes the zenith angle. In equation (1) N denotes the maximum ion density for the layer and that is calculated from the familiar equation

$$N = 1.24 \times 10^4 f^2 \quad (3)$$

when f is measured in megacycles per sec. During the eclipse, we have

$$\frac{dN}{dt} = rq - \alpha N^2 = r q_0 \cos\psi - \alpha N^2 \quad (4)$$

where r denotes the fraction of the solar disk not covered by the moon at time t . To facilitate calculations, we change dN/dt into $\Delta N/\Delta t$ where Δt represents an interval of about 15 minutes. Berkner and Seaton³ used this approximation and derived the following expression:

$$N_2 = (N_1 + q_0 \bar{f}(z) \Delta t) / (1 + N_1 \alpha \Delta t) \quad (5)$$

They found this approximation follows the theoretical curve very closely. We have therefore adopted Berkner and Seaton's formula for our work with the following modification to suit eclipse conditions:

$$\bar{f}(z) = \frac{r_1 \cos\psi_1 + r_2 \cos\psi_2}{2}, \quad (6)$$

2. E. O. Hulbert, *Phys. Rev.* **55** (1939), 646.
3. Berkner and Seaton, *Terr. Mag.* **45** (1940), 393.

where r_1 and r_2 are fractions of solar disk exposed at times t_1 and t_2 . For a normal day, r is equal to unity of course.

In our calculations, N_1 is fixed at 15.3×10^5 ions per cm^3 and is calculated from equation (3) from the observed critical frequency of 11.1 Mc/sec at 0826 120° EMT on the day of eclipse. N_2 , the maximum ion density at t_2 or end of Δt , is calculated with the aid of equation (5) when $f(z)$, q_0 and α are also known. In equation (5) the interval between observations Δt is measured in seconds, $f(z)$ is derived from equation (6), q_0 and α are obtained from solving the simultaneous equations (1) and (4) for twelve different times by taking values of $\Delta N/\Delta t$, N , r , and $\cos \phi$ from the control data and eclipse data at the corresponding times. The values so obtained are

$$q_0 = (1.97 \pm .24) \times 10^3 \text{ ion-electron pairs/cm}^3 \text{ per sec}$$

$$\alpha = (4.05 \pm .66) \times 10^{-10} \text{ cm}^3/\text{electron per sec.}$$

In our calculations we have adopted $q_0=2000$ and $\alpha=4 \times 10^{-10}$ in producing the theoretical curves for fig. 1. To give an example of our calculations, we show in Table 1 the pertinent data for the theoretical curve showing the eclipse effect.

TABLE 1

Time in 120°EMT	N_1 $\times 10^5$	$q_0 f(z) \Delta t$ $\times 10^5$	$1 + N_1 \alpha \Delta t$	N_2 $\times 10^5$	Frequency Calculated Mc/sec.	Frequency Observed Mc/sec.
0826	15.3	9.2	1.52	16.2	11.1	11.1
0840	16.2	7.7	1.51	15.9	11.5	11.2
0853	15.9	8.5	1.65	14.8	11.3	11.4
0910	14.5	5.6	1.57	13.6	10.9	10.6
0926	13.6	3.5	1.48	11.6	10.5	11.2
0940	11.6	2.0	1.25	10.9	9.7	10.3
0950	10.9	7.0	1.51	11.8	9.4	9.9
1009	11.8	9.2	1.45	14.5	9.8	10.0
1025	14.5	11.7	1.52	17.2	10.8	11.5
1040	17.2	8.8	1.39	18.7	11.8	11.9
1050	18.7	16.1	1.70	20.5	12.3	12.0
1105	20.5	16.7	1.74	21.4	12.9	12.9
1120	21.4				13.2	14.3

There are a number of discontinuities both for the control curve and for the eclipse curve. Some of the smaller variations may be due to errors of observation but the larger ones must be accounted for in other ways.

Referring to the observed eclipse curve, there is a definite rise and fall between 0740 and 0825, the beginning of the optical eclipse. At 0853 there is a significant drop followed by a larger rise at 0910. After the eclipse maximum, there is a sharp rise at 1009 and a smaller one at 1025. The increases in frequency is rather important for they represent increases in ionization and there must be special agents producing them. In analyzing F-1 layer ionization during the same eclipse which took place at Wakkanai (45°N , 142°E), Japan about an hour later than ours, Nakata⁴ identified two upward departures from a smoothed curve as being due to solar eruptions at 0958 and 1017 120° EMT as observed by the Tokyo Astronomical Observatory. Our data are lacking from 0905 to 1009 for reasons already stated, but the curve does show a marked rise at 1009 and a lesser one at 1025. Most probably they are due to the same solar eruptions. As to the other discontinuities, they may be due to radiations from coronal regions or streamers as postulated by Wells and Shapley⁵. But lacking astronomical information, we are not prepared to discuss them.

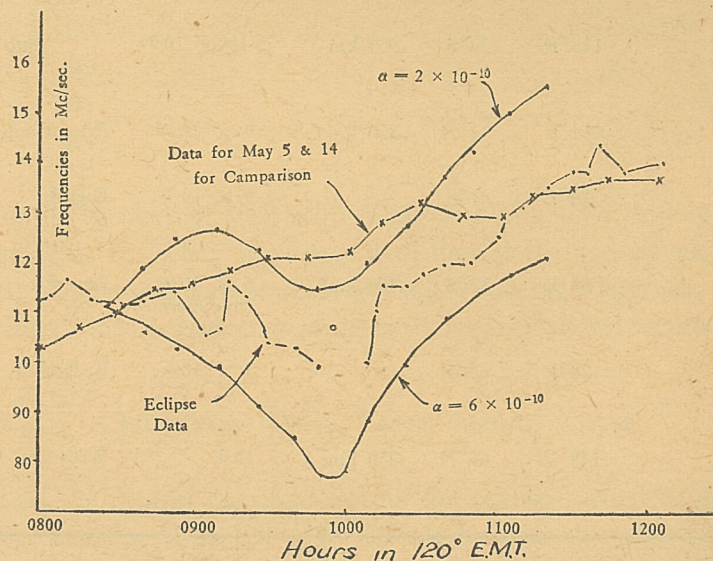


Fig. 2. Showing how the theoretical curves deviate from the eclipse data when the coefficient of recombination is made slightly bigger or smaller than $\alpha = 4 \times 10^{-10} \text{ cm.}^3/\text{electron per sec.}$

In figure 2, we have drawn the computed curves in terms of $\alpha=2$ and 6×10^{-10} respectively, keeping $q_0=2000$. It is seen that the lower value for

4. Y. Nakata, *Rep. of Ionosphere Res. in Japan*, **4** (1950), 21.

5. H. W. Wells and A. H. Shapley, *Terr. Mag.* **51** (1946), 401.

the coefficient of recombination yields a curve too high and the higher value a curve too low to fit the observed eclipse data.

For the sake of comparison we list here below in Table II the values for the effective coefficient of recombination as determined by other workers whose reports are available to us:

Table II.—Coefficient of Recombination for F-2 Layer

Place & Time of Eclipse	Long.	Lat.	Minimum Virtual Height	Coef. of Recombination	Authority
Patos, Brazil Oct. 1, 1950	42°W	7°S		10^{-10}	Gilliland ⁶
Bébédouro, Brazil, May 20, 1947	?	?		10^{-10}	Denisse, Seligmann, ⁷ Gallet
Huancayo, Peru, Jan. 25, 1944	75°W	12°S	320 km	2.5×10^{-10}	Wells and Shapley ⁵
Watheroo, Australia, Aug. 1, 1943	116°E	30°S	300 km	5.10×10^{-10}	ditto
Wuchang, May 9, 1948	114°E	31°N	300 km	4×10^{-10}	Present authors
Victoria W. S. Africa Oct. 1, 1940	24°E	31°S		4×10^{-10}	Higgs ⁸
Queenstown, South Africa Oct. 1, 1940	27°E	32°S	450 km*	6×10^{-11} (minimum value)	Pierce ⁹
Sörmjöle, Sweden, July 9, 1945	20°E	64°N		3×10^{-9}	Rydbeck ¹⁰
College, Alaska, Feb. 4-5, 1943	148°W	65°N	250 km	10^{-9}	Wells and Shapley ⁵

*extrapolated from Pierce's diagrams by present authors.

We have arranged the locations in the order of increasing latitude for there seems to be a general tendency for α to increase as we approach the higher latitudes. This is especially evident in the case of Sörmjöle, Sweden

6. T. R. Gilliland, *Sci. Abst. Sec. A*, **45** (1942), 277.

7. *URSI*, **7** (1949), 240.

8. A. J. Higgs, *Nature* **149** (1942), 701; *Wireless Engineer* (1943), No. 2938.

9. J. A. Pierce, *Proc. I.R.E.* **36** (1948), 8.

10. *URSI*, **7** (1949), 239.

and College, Alaska. The only clear departures are the values given by Higgs and Pierce, both reporting on the 1940 South African Eclipse. Pierce mentioned that he was giving the minimum value for α and the F-2 layer virtual height at the beginning of the eclipse as extrapolated by us was abnormally high—450 km. Higgs was most probably observing under similar conditions. As Wells and Shapley⁵ pointed out in their study of eclipse data at Huancayo, Watheroo and College, the value of the coefficient of recombination is related to the minimum virtual height and ion density—the greater values of α being associated with lower heights and lower ionic density.

In a recent article, Savitt¹¹ studied the eclipse effects of May 20, 1947, over Bocayuva, Brazil. He found α was different at different virtual heights and gave as the values of α at various levels as follows:

Minimum Virtual Height	Coeff. of Recombination
220 km	3×10^{-9}
260 „	1×10^{-9}
300 „	4×10^{-10}
320 „	2.5×10^{-10}

Savitt's results check very well with Wells and Shapley's findings as can be seen from Table II. They also agree with that of the present authors. Since the virtual heights and ion densities are smaller at high latitudes, the general trend of increasing α with increasing latitudes is what we would expect.

THICKNESS OF F-2 LAYER DURING ECLIPSE

Both on the control days and during the eclipse, virtual height measurements were made at $f_0F2 - 1.5, -3.0, -4.5$ Mc respectively, where f_0F2 signifies the F-2 layer critical frequency for the ordinary ray. By assuming the validity of Booker and Seaton's¹² assumption that the variation of ion density with height may be represented by a parabola, we deduce the real height (or height of maximum ion density in the layer) as equal in magnitude to the virtual height at a frequency equal to 0.834 of f_0F2 . The minimum

11. Jacob Savitt, *J. Geophys. Res.*, **55** (1950), 385.

12. Booker and Seaton, *Phys. Rev.*, **57** (1940), 87.

virtual height is obtained by interpolation from the curve as determined by the three points mentioned above.

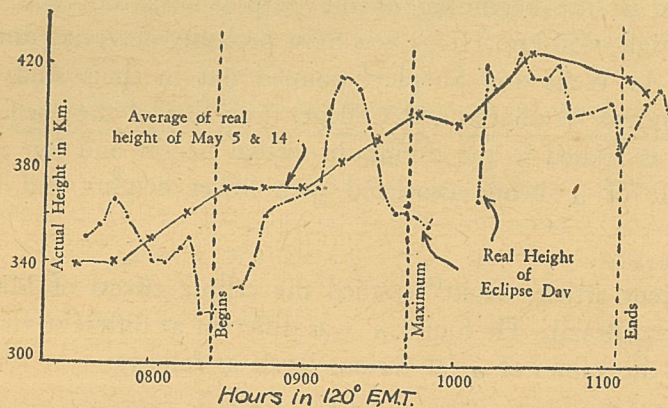


Fig. 3. The variation of Real Height during Eclipse and on control days—average of May 5 and 14. There is a Distinct Drop in Real Height near Eclipse Maximum.

In fig. 3 we have plotted the real height curves during the eclipse and for the control days (without correcting for retardation in the *E* and *F*-1 layers). The curve rises when the eclipse begins, then it drops just before and during the eclipse and after that it rises to approach the control curve. In general on the eclipse day, the real height curve runs parallel to the frequency practically in synchronism, which can be seen by comparing fig. 3 with fig. 1.

Both the real height and the minimum virtual height are plotted in fig. 4; the distance between the two curves therefore represents the half thickness of the *F*-2 layer. The top figure shows the thickness during eclipse and the lower figure that for the control days. The layer seems to be compressed during the eclipse. The whole layer rises with the first contact, drops to a minimum at eclipse maximum, then recovers normalcy.

Reporting on the 1940 South African Eclipse, Pierce⁹ observed depression of virtual height surface when the eclipse began, followed by a recovery rise. He attributed the lowering of the virtual height to the cooling of the upper atmosphere in the shadow of the moon with consequent increases in layer density. Our results also show a lowering of the layer during eclipse maximum. The rise of the layer at the beginning of the eclipse that we observed was not present in the South African eclipse. It might have been caused by accidental atmospheric tides.

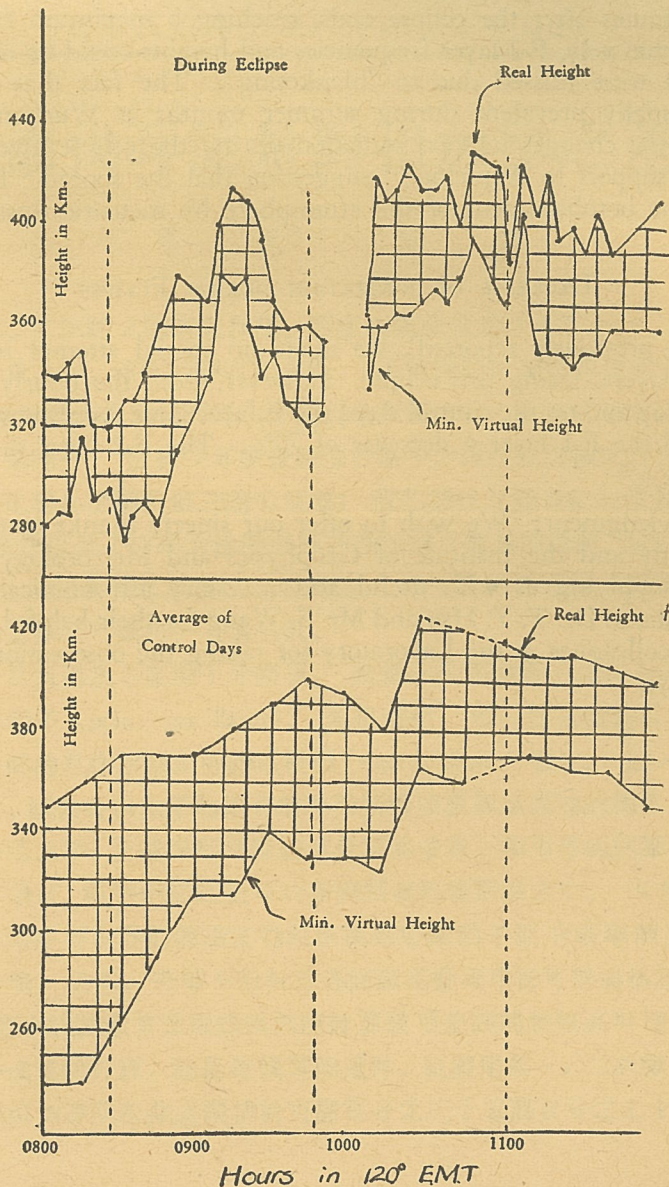


Fig. 4. Comparing the Half-thickness of F_2 -region during Eclipse and on Control Days

SPORADIC E IONIZATION

During the eclipse, sporadic E was prevalent. Commencing about 12 minutes after the first contact, it remained almost without any intermission till

some 38 minutes after the eclipse ends, reaching a maximum frequency of 12 Mc. Fortunately, F-2 layer frequencies and heights could be observed and no readings were missed due to "blanketing". The fact that sporadic E, which is usually prevalent during summer months at Wuchang, was not affected by the changes in solar radiation during the eclipse gives one more instance of support to Appleton's¹³ suggestion that the sporadic E ionization is due to the bombardment of the atmosphere by meteoric dust.

DECREASE OF IONIZATION DURING ECLIPSE

As was previously reported¹, we made no special attempt to study the E and F-1 layers during this eclipse. However, from the hourly records on the eclipse day and on the control days, the E layer ionization shows a decrease of 60% and the F-1 layer a decrease of 70%. The F-2 layer shows a drop of about 31%.*

Acknowledgment: We wish to offer our sincere thanks to the Institute of Astronomy and the Institute of Geophysics and Meteorology, Academia Sinica for supplying us with useful and necessary astronomical, solar and magnetic data, to Dr. T. Y. Hsu and Mr. S. Wang for their helpful discussions, and to our colleagues in the Laboratory for taking the observations and help in other ways.

13. E. V. Appleton and R. Naismith, *Proc. Phys. Soc.* **59** (1947), 461.

*This is slightly less than our previous value of 36% on account of elimination of disturbed days from control curve.